

CT-Definable Subtypes of Chronic Obstructive Pulmonary Disease: A Statement of the Fleischner Society¹

David A. Lynch, MB
John H. M. Austin, MD
James C. Hogg, MD, PhD
Philippe A. Grenier, MD
Hans-Ulrich Kauczor, MD
Alexander A. Bankier, MD
R. Graham Barr, MD
Thomas V. Colby, MD
Jeffrey R. Galvin, MD
Pierre Alain Gevenois, MD, PhD
Harvey O. Coxson, PhD
Eric A. Hoffman, PhD
John D. Newell, Jr, MD
Massimo Pistolesi, MD
Edwin K. Silverman, MD, PhD
James D. Crapo, MD

The purpose of this statement is to describe and define the phenotypic abnormalities that can be identified on visual and quantitative evaluation of computed tomographic (CT) images in subjects with chronic obstructive pulmonary disease (COPD), with the goal of contributing to a personalized approach to the treatment of patients with COPD. Quantitative CT is useful for identifying and sequentially evaluating the extent of emphysematous lung destruction, changes in airway walls, and expiratory air trapping. However, visual assessment of CT scans remains important to describe patterns of altered lung structure in COPD. The classification system proposed and illustrated in this article provides a structured approach to visual and quantitative assessment of COPD. Emphysema is classified as centrilobular (subclassified as trace, mild, moderate, confluent, and advanced destructive emphysema), panlobular, and paraseptal (subclassified as mild or substantial). Additional important visual features include airway wall thickening, inflammatory small airways disease, tracheal abnormalities, interstitial lung abnormalities, pulmonary arterial enlargement, and bronchiectasis.

©RSNA, 2015

¹From the Departments of Radiology (D.A.L.) and Medicine (J.D.C.), National Jewish Health, 1400 Jackson St, Denver, CO 80206; Department of Radiology, Columbia University, New York, NY (J.H.M.A.); Department of Pathology, University of British Columbia, Vancouver, BC, Canada (J.C.H.); Department of Radiology, Hôpital Pitié-Salpêtrière, Paris, France (P.A.G.); Department of Diagnostic and Interventional Radiology, University of Heidelberg, Heidelberg, Germany (H.U.K.); Department of Radiology, Beth Israel Deaconess Medical Center, Boston, Mass (A.A.B.); Departments of Medicine and Epidemiology, Columbia University Medical Center, New York, NY (R.G.B.); Department of Pathology, Mayo Clinic Scottsdale, Scottsdale, Ariz (T.V.C.); Department of Chest Imaging, American Institute for Radiologic Pathology, Silver Spring, Md (J.R.G.); Department of Radiology, Hôpital Erasme, Brussels, Belgium (P.A.G.); Department of Radiology, Vancouver General Hospital, Vancouver, BC, Canada (H.C.); Department of Radiology, Division of Physiological Imaging, Carver College of Medicine, University of Iowa Hospitals and Clinics, Iowa City, Iowa (E.A.H., J.D.N.); Respiratory Unit, Department of Experimental and Clinical Medicine, University of Florence, Florence, Italy (M.P.); and Channing Laboratory, Brigham and Women's Hospital, Boston, Mass (E.K.S.). Received July 16, 2014; revision requested September 2; revision received October 28; accepted November 24; final version accepted February 16, 2015. Address correspondence to D.A.L. (e-mail: lynchd@njhealth.org).

©RSNA, 2015

The term *chronic obstructive pulmonary disease* (COPD), currently defined on the basis of spirometric evidence of airway obstruction, encompasses several distinct but overlapping obstructive syndromes, including emphysema, chronic bronchitis, and reversible or irreversible small airways obstruction (1). The Global Obstructive Lung Disease (GOLD) system has been widely used to identify and classify the severity of postbronchodilator airflow limitation in COPD, with GOLD stage I referring to subjects with a ratio of forced expiratory volume in 1 second (FEV_1) to forced vital capacity (FVC) of less than 0.7 but with preserved FEV_1 , and GOLD stages II, III, and IV when the FEV_1/FVC ratio is less than 0.7 and FEV_1 is less than 80%, 50%, and 30% of predicted, respectively (2). Individuals with identical GOLD stages may have different morphologic appearances at computed tomography (CT) (3). Some have extensive emphysema, whereas others with equal functional impairment have an airway-dominant phenotype with little or no emphysema. These morphologic differences may reflect important differences in the underlying pathophysiology and genomic profile of COPD. Furthermore, individual subtypes of emphysema may have different pathophysiologic importance. For example, Smith et al (4) showed that smokers with predominantly centrilobular emphysema (CLE) had a higher level of cigarette exposure, higher lung volumes, and lower lung diffusing capacity than those without emphysema. Conversely, smokers with a predominantly “panlobular” pattern of emphysema had a relatively lower body mass index than smokers without emphysema.

In addition, morphologic changes of emphysema and airways disease are found in a substantial proportion of subjects who do not meet the spirometric

criteria for COPD (5). Standardized characterization of COPD and other smoking-related lung changes at CT is particularly important given the emerging role of reduced-dose CT in screening for lung cancer in cigarette smokers (6).

COPD is associated with irreversible structural pulmonary changes, including parenchymal destruction (emphysema), large airway remodeling, and reduction in the caliber and number of small airways in the lung (7). CT is a well-validated technique to visually and quantitatively assess the in vivo presence, pattern, and extent of emphysema (8–11). Bronchial wall thickness and the extent of emphysema at quantitative CT in patients with COPD are independent determinants of the degree of airflow obstruction at pulmonary function testing (12) and the risk of COPD exacerbations (13). Emphysema assessed quantitatively is also associated with increased all-cause mortality in patients with COPD (14). Quantitative CT assessment of expiratory gas trapping is emerging as a powerful predictor of the severity of airway obstruction in COPD (12,15,16). Furthermore, the observation that expiratory gas trapping correlates only weakly with histologic severity of emphysema strongly suggests that it is caused by obstruction in the smaller airways rather than emphysema (17). Quantification of low-attenuation areas, expiratory gas trapping, and airway wall thickness can help define specific COPD phenotypes with differing clinical and physiologic features (18).

The purpose of this statement is to define the phenotypic abnormalities recognizable at visual and quantitative evaluation of CT images in subjects with COPD. Although these abnormalities often overlap, we believe that identification and quantification of the predominant morphologic findings and their grouping into defined subtypes of COPD

will improve diagnostic accuracy, help optimize treatment, facilitate genetic analysis, and provide a framework for data comparison in clinical trials. Given the focus on COPD and related phenotypes, discussion of other smoking-related lung conditions such as pulmonary Langerhans cell histiocytosis, lung cancer, and usual interstitial pneumonia is beyond the scope of this article. Although COPD unrelated to smoking (eg, COPD related to biomass fuel exposure) is not discussed herein, the same concepts likely apply to these conditions.

Technical Approach

CT Image Acquisition and Evaluation

CT is currently the most widely available and precise imaging method for the characterization of COPD. Chest radiography does not allow accurate morphologic assessment of COPD owing to

Published online before print

10.1148/radiol.2015141579 Content codes: **CH** **CT**

Radiology 2015; 000:1–14

Abbreviations:

CLE = centrilobular emphysema
 COPD = chronic obstructive pulmonary disease
 FEV_1 = forced expiratory volume in 1 second
 FVC = forced vital capacity
 GOLD = Global Obstructive Lung Disease
 PLE = panlobular emphysema
 PSE = paraseptal emphysema

Author contributions:

Guarantors of integrity of entire study, D.A.L., J.D.C.; study concepts/study design or data acquisition or data analysis/interpretation, all authors; manuscript drafting or manuscript revision for important intellectual content, all authors; manuscript final version approval, all authors; agrees to ensure any questions related to the work are appropriately resolved, all authors; literature research, D.A.L., J.H.M.A., P.A.G., H.U.K., A.A.B., R.G.B., T.V.C., J.R.G., P.A.G., H.C., E.A.H., J.D.N., M.P., J.D.C.; clinical studies, D.A.L., J.H.M.A., P.A.G., H.U.K., E.K.S., J.D.C.; statistical analysis, J.D.C.; and manuscript editing, D.A.L., J.H.M.A., J.C.H., P.A.G., H.U.K., A.A.B., R.G.B., T.V.C., P.A.G., H.C., E.A.H., J.D.N., M.P., E.K.S., J.D.C.

Funding:

This research was supported by grants R01 HL089897 and R01 HL089856 from the National Heart, Lung, and Blood Institute.

Conflicts of interest are listed at the end of this article.

Advance in Knowledge

- Visually based classification of the CT appearances in chronic obstructive pulmonary disease (COPD) provides complementary information to quantitative CT.

Implication for Patient Care

- Combined quantitative and visual assessment of CT may contribute to improved personalized care of patients with COPD.

limited resolution and superimposition of overlapping structures. Although magnetic resonance (MR) imaging, particularly with use of hyperpolarized gases, offers exciting possibilities for measuring alveolar dimensions (19–23), technical issues currently limit wide acceptance. With advances in fluorine MR imaging, some of these limitations may be eliminated (24). Other potentially promising MR imaging techniques, such as ultrashort echo time pulse sequences, oxygen-enhanced MR imaging, or the use of fluorinated gases, require validation in multicenter studies.

The appropriate CT technique for the evaluation of COPD should optimize visual assessment of the lung structure for emphysema and airways disease and help identify other complications of cigarette smoking, such as lung cancer, lung fibrosis, and Langerhans cell histiocytosis. Moreover, CT should facilitate quantitative evaluation of emphysema and airway wall thickening while using the minimum possible radiation dose. CT images should be viewed at window level settings suitable for lung evaluation (typically a window level of -700 HU and window width of 1500 HU). A narrower window width (750 – 1000 HU) may be useful for detecting or excluding early emphysema (25). Minimum intensity projections may help show the presence and extent of emphysema (26). Standard images from subjects with normal and abnormal findings may improve observer agreement in the visual characterization of CT changes (27).

Unenhanced volumetric thin-section CT is generally recommended for COPD characterization (28). Precise scanner calibration, ideally with a standardized CT phantom (29), is important for ensuring the accuracy of CT numbers (30,31). Scanner-specific protocols have been designed to compare quantitative CT indexes of parenchymal and airway status (32). A high-spatial-resolution reconstruction algorithm is better for visual assessment of the lungs (28), whereas a smoother reconstruction algorithm facilitates computerized analysis by reducing image noise (33,34). Submillimeter z-axis

resolution, with overlapping section reconstructions, is recommended for optimal airway analysis (35,36). Expiratory CT, performed at functional residual capacity or at residual volume, is a powerful tool for determining the severity of airway obstruction in cigarette smokers (12,16,37,38) and can suggest tracheobronchomalacia, although this condition is better shown with dynamic expiratory imaging (39). In the absence of lung volume control with a pneumotachometer (40,41), it is critically important for the CT technologist to rehearse breathing instructions with the patient, encouraging a full deep inspiration to total lung capacity for the inspiratory acquisition and expiration to functional residual capacity or residual volume for the expiratory acquisition (42).

The CT radiation dose level used for the evaluation of COPD is driven by the balance between radiation dose and image quality. Adequate visual characterization can be achieved with reduced-dose CT acquisition techniques, as used for lung cancer screening (43,44). Excessive image noise with a reduced CT dose can simulate emphysema, particularly at quantitative CT (45,46), and may impair segmentation of the airways and quantitative evaluation of airway wall thickness. Given the older age profile of subjects with COPD and the importance of acquiring precise quantitative information, moderate radiation doses (<10 mSv) are probably acceptable. However, as CT detector technology and image reconstruction methods evolve, in combination with improvements in quantitative CT, it is likely that the required CT dose will further decrease. Several large multicenter studies (4,47–50) have used a range of settings for key scan acquisition parameters, and these are summarized in the Table. Expiratory CT may be performed with lower radiation exposure (tube current ≤ 50 mAs) because it is primarily used to quantify air trapping (51). Iterative reconstruction techniques are not currently recommended because the effects on quantitative and visual evaluation are uncertain at the time of writing (37,52).

CT Techniques Used for Visual and Quantitative Evaluation of COPD

Parameter	Value
Detector configuration	≥ 16 detectors
Pitch	1–1.4
Acquisition collimation (mm)	≤ 1
Kilovolt peak	120
Effective milliamperes second	40–200
Reconstruction algorithms	Smooth and sharp
Reconstruction section thickness (mm)	0.625–1
Reconstruction interval (mm)	0.5–0.9
Reconstruction field of view	Lungs only

Quantitative CT Image Analysis

The goals of quantitative CT in COPD are to quantify the presence and percentage of emphysema-like lung (low-attenuation areas), the lobar and zonal distribution of the low-attenuation regions, changes in airway walls and luminal caliber, and the severity of gas trapping at expiratory CT. A number of analysis platforms are available as commercial software and in academic institutions (36,53–55). A detailed discussion of quantitative CT methodology is beyond the scope of this article, but further details are available in recent review articles (54,56–58). Although quantitative CT provides useful information regarding emphysema, airways, and air trapping and provides a means of objectively characterizing and following these pathologic processes, visual assessment of CT scans remains important to describe patterns of altered lung structure in COPD and provides distinct phenotypes not currently identified with quantitative CT.

Visually Defined Subtypes of COPD

Figure 1 lists the visually defined phenotypes of emphysematous destruction as well as the airway changes seen in COPD. Figure 2 illustrates the gross abnormality and micro-CT features of the primary lesions of each of the major emphysematous phenotypes of COPD.

Figure 1

Emphysema***1. Centrilobular Emphysema:** the dominant pattern should be scored

- a. Trace Centrilobular Emphysema (CLE):** minimal centrilobular lucencies, occupying < 0.5% of a lung zone.
- b. Mild CLE:** scattered centrilobular lucencies, usually separated by large regions of normal lung, involving an estimated 0.5-5% of a lung zone.
- c. Moderate CLE:** many well-defined centrilobular lucencies, occupying more than 5% of any lung zone.
- d. Confluent CLE:** coalescent centrilobular or lobular lucencies, including multiple regions of lucencies that span several secondary pulmonary lobules, but not involving extensive hyperexpansion of secondary pulmonary lobules or distortion of pulmonary architecture.
- e. Advanced Destructive Emphysema (ADE):** panlobular lucencies, with hyperexpansion of secondary pulmonary lobules and distortion of pulmonary architecture.

2. Panlobular Emphysema

Associated with A1AT Deficiency: most commonly, a lower lobe predominant pattern involving generalized destruction of all acini more or less equally.

3. Paraseptal Emphysema

- a. Mild Paraseptal Emphysema (PSE):** small (≤ 1 cm), well-demarcated rounded juxtapleural lucencies, aligned in a row along a pleural margin, sometimes including along an interlobar fissure, and sometimes including a few small rounded lucencies immediately central to the juxtapleural lucencies.
- b. Substantial Paraseptal Emphysema:** mainly large (>1 cm diameter) juxtapleural cyst-like lucencies or bullae, involving more than the lung apices, aligned in a row along a pleural margin, and sometimes including adjacent to an interlobar fissure.

Airway Disease

Airway disease is commonly found with all forms of emphysema, but also commonly occurs in the absence of emphysema as a predominant expression of COPD.

- 1. Bronchial Disease:** Thickening of walls of segmental and subsegmental airways.
- 2. Small Airway Disease (SAD):** Inflammatory SAD can be directly identified on CT scan by the presence of peripheral centrilobular micronodular opacities. Obstructive SAD is identified by gas trapping on expiratory CT, or FEV1/FVC ratio < 0.7, in the absence of significant emphysema.

Associated Features

- 1. Large Airway Disease:** Tracheobronchomalacia, saber sheath trachea, tracheobronchial outpouching/diverticula.
- 2. Interstitial Lung Abnormality:** Patchy ground glass abnormality, mild subpleural reticular abnormality.
- 3. Pulmonary Arterial Enlargement:** Enlargement of the pulmonary artery, suggesting pulmonary hypertension, occurs in advanced COPD, and a ratio of the pulmonary artery diameter to the aorta diameter >1 has been associated with increased risk of COPD exacerbation.
- 4. Bronchiectasis**

Figure 1: Visually defined patterns of COPD at CT. * = If there are fewer than four to five small (≤ 1 cm) juxtapleural circumscribed areas of lucency in the apex of a lung, ignore. A1AT = α_1 -antitrypsin.

CLE

McLean in Australia (59–62) and Leopold and Gough in the United Kingdom (63) provided the first pathologic descriptions of CLE and showed that the primary lesion is produced by dilation and destruction of respiratory bronchioles within a single acinus. Furthermore, they both demonstrated that the centrilobular lesions are formed by coalescence of several primary lesions. Subsequently, the destruction spreads to the entire lung lobule and fuses many destroyed lobules together to produce a

pattern of coalescent destruction that sometimes disintegrates to form large bullous lesions. By performing three-dimensional reconstructions of serial histologic sections of 90 individual centrilobular spaces, Leopold and Gough (63) showed that all CLE lesions had a supplying bronchiole lined with abnormal epithelium that was associated with varying degrees of airway wall thickening and lumen narrowing. In addition, they also described widespread evidence of bronchiolitis ranging from active cellular infiltration to fibrosis. In a subsequent

study, they used fine particulate lead dust bronchograms to confirm that some centrilobular spaces filled easily from the conducting airways and suggested that the pathways between the mainstem bronchus and the centrilobular spaces were shorter in those with emphysema than in normal airways (64). Others used this same technique to visualize CLE, showing that the areas of CLE are hypercompliant and reach their maximum volume at very low transpulmonary pressures and that the resistance to collateral ventilation falls to very low levels

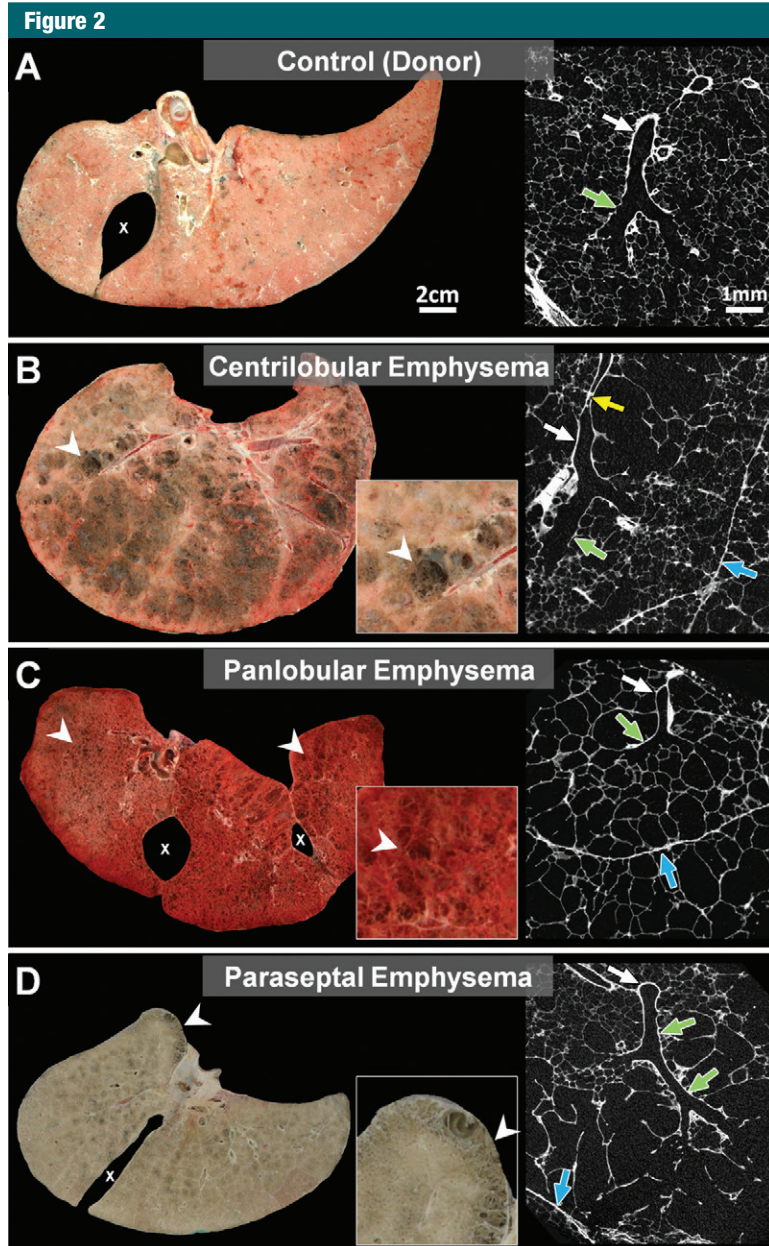


Figure 2: Comparison of frozen lung slices and micro-CT images from, *A*, donor (control) lung to lungs affected by, *B*, centrilobular, *C*, panlobular, or, *D*, paraseptal phenotypes of emphysematous destruction. *A*, Micro-CT image of control lung shows a terminal bronchiole (white arrow) connecting to respiratory bronchiole (green arrow) supplying alveoli of normal size. *B*, Extensive centrilobular destruction (arrowheads) is seen in lung slice, and micro-CT scan of primary lesion shows dilatation and destruction of proximal respiratory bronchioles (green arrow), with sparing of alveoli near lobular septa (blue arrow). Moreover, terminal bronchiole leading into centrilobular lesion is narrowed (yellow arrow) and then opens up again (white arrow), a feature that can be better appreciated in video associated with the article by McDonough et al (7). *C*, In contrast, the panlobular phenotype of emphysema in this case of α_1 -antitrypsin deficiency shows relatively mild destruction of gross specimen (arrowheads), and micro-CT scan shows uniform destruction of alveoli extending right up to lobular septa (blue arrow). Terminal bronchiole (white arrow) and respiratory bronchiole (green arrow) are normal. *D*, Paraseptal phenotype of emphysema shows typical lesions (arrowheads) beneath pleural surface on gross specimen, and micro-CT scan shows that alveoli adjacent to lobular septa are dilated and destroyed, with sparing of center of lobule. Terminal bronchiole (white arrow) and respiratory bronchiole (green arrow) are normal. Images from control lung and lung affected by PSE came from organ donors and were released for research when judged to be unsuitable for transplantation, whereas lungs affected by CLE and panacinar emphysema were donated by patients treated by means of lung transplantation. The protocol for the preparation of the specimens is fully described in reference 7. *x* on *A*, *C*, and *D* indicates interlobar fissure(s).

in regions of emphysematous destruction (65). More recent studies based on micro-CT confirmed earlier observations that the supplying bronchioles often follow a tortuous pathway to reach the centrilobular space (7) (see video in article by McDonough et al [7]). More importantly, they also showed a remarkable reduction in the total number of terminal bronchioles per lung, from 22300 ± 3900 per adult human lung in control

subjects to 2400 ± 600 per lung when CLE was present. This study provided histologic evidence that it was surviving airways with thickened walls (see figure 4 in the article by Klein et al [5]) that supplied the terminal bronchioles. Most importantly, micro-CT measurements showed that the reduction in terminal bronchioles occurred before the onset of emphysematous destruction. Collectively, these data support the hypothesis

that bronchiolitis is the earliest lesion in COPD and suggest that CLE is formed distal to surviving bronchioles, supported by collateral ventilation of acini within the same lobule that lost terminal bronchioles (7).

At CT, CLE is characterized by small well-defined or poorly defined areas of low attenuation surrounded by normal lung. Centrilobular pulmonary arteries or arterioles, which are often seen traversing the hypoattenuated areas, mark the center of each lobule (9). This pattern of emphysema correlates well with pathologically demonstrated CLE (59,66–68) and with micro-CT measurements of the primary lesions (Fig 2, *B*). This is the most common type of smoking-related emphysema and is usually upper lung predominant (Figs 3, 4). The low-attenuation areas may range

Figure 3



Figure 3: Mild CLE. CT scan in patient with GOLD stage I COPD shows scattered centrilobular lucencies, separated by large regions of normal lung, involving an estimated 0.5% of upper lung zone.

Figure 4

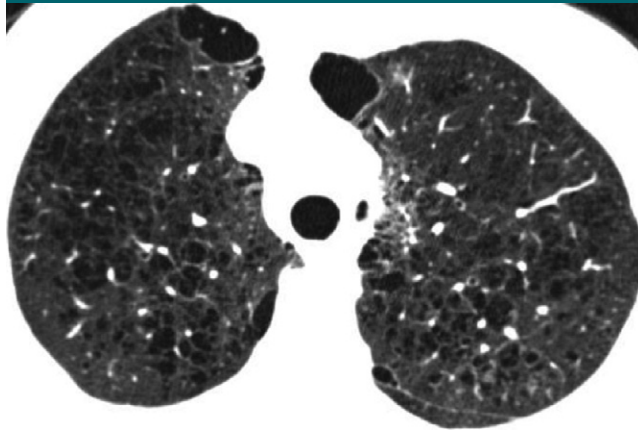


Figure 4: Moderate CLE. CT scan in patient with GOLD stage I COPD shows many well-defined centrilobular lucencies that occupy more than 5% of upper lung zone. PSE is seen in antero-medial right and left lungs.

Figure 5

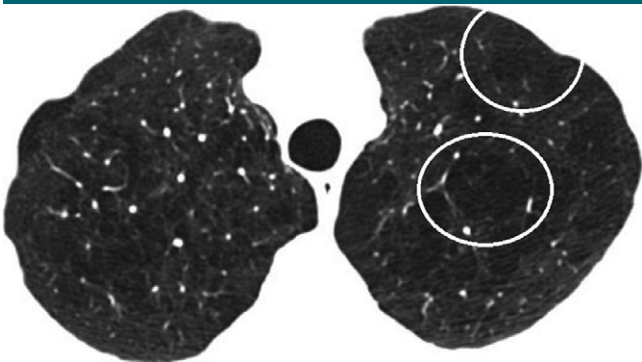


Figure 5: Confluent CLE. CT scan in patient with GOLD stage I COPD shows multiple lucencies that span several secondary pulmonary lobules (circled in left lung) but are not associated with extensive hyperexpansion of secondary pulmonary lobules or distortion of pulmonary architecture.

Figure 6

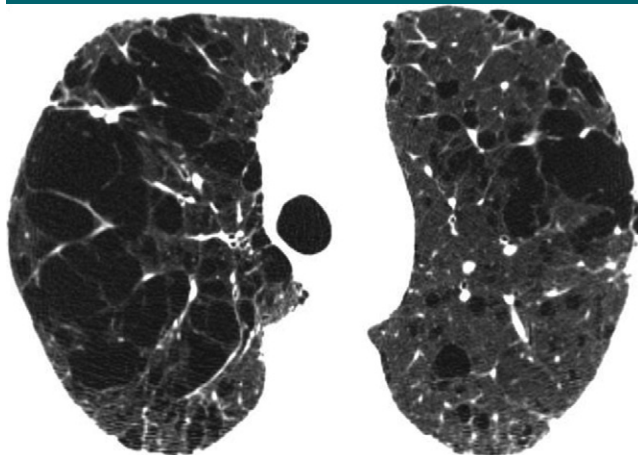


Figure 6: Advanced destructive emphysema. CT scan in patient with GOLD stage I COPD shows hyperexpansion of secondary pulmonary lobules with distortion of pulmonary architecture.

from less than 1 mm to more than 3 cm in diameter.

Severe Emphysema

Confluent emphysema.—As CLE becomes more severe, the areas of low attenuation become confluent (Fig 5) and the centrilobular distribution becomes less apparent. In most cases, the areas of low attenuation have no visible walls; however, very thin walls may be seen—particularly when the areas of emphysema are extensive. The apparent walls

in such cases probably represent atelectasis or interlobular septa adjacent to the emphysematous spaces. Confluent emphysema may be differentiated from advanced destructive emphysema by the presence of a preserved rim of normal lung attenuation intervening between areas of lung destruction, and by the absence of lobular hyperexpansion, architectural distortion, or splaying of decreased caliber of vessels.

Advanced destructive emphysema.—Advanced destructive emphysema is

manifested as a generalized decrease of attenuation of the lung without focal hypoattenuation (Fig 6) and represents an advanced stage of CLE. Interlobular septa are often preserved and splayed, facilitating the identification of pulmonary lobular hyperexpansion. In addition, the more central pulmonary vessels are often distorted, splayed, and narrowed with decreased branching (architectural distortion). Although this pattern may be indistinguishable at CT from the panlobular pattern described



Figure 7: PLE related to α_1 -antitrypsin deficiency. CT scan through lower lungs shows widespread confluent areas of hyperlucency spanning one or several lobules. Some lobules, outlined by intact interlobular septa, appear hyperexpanded (arrowheads).

below, and the term *panlobular* has been previously used to describe this entity (4,69), we prefer to use the term *advanced destructive emphysema* because it may not represent histologic panlobular emphysema (PLE).

PLE

PLE specifically refers to diffuse emphysematous destruction across the lobule (Fig 2, C). Wyatt et al (70) first described this pattern, which was subsequently linked to low circulating levels of α_1 -antitrypsin (71). It is now known that low levels of α_1 -antitrypsin are produced by a genetic defect in the α_1 -antitrypsin gene that causes the protein to misfold after it is produced, causing it to accumulate in liver cells, where it stimulates inflammation and subsequent cirrhosis without being secreted into the circulating blood (72). In general, the extent and severity of alveolar destruction in PLE is milder than that in CLE, but it affects all of the acini within a lung lobule more or less equally (see the gross pathology and micro-CT images of the primary lesion in Fig 2, C).

PLE has also been reported in the absence of α_1 -antitrypsin deficiency (73), including in intravenous drug abuse (74). In cigarette smokers,

mixtures of PLE and CLE can be found within the same lungs (69). Under these conditions, Kim et al (69) have suggested that PLE is less likely to be associated with small airway obstruction than CLE. However, micro-CT studies of α_1 -antitrypsin deficiency indicate that both CLE and PLE are associated with narrowing and destruction of the terminal bronchioles in end-stage COPD (7).

At CT, advanced PLE in association with α_1 -antitrypsin deficiency often occurs in a lower lobe–predominant distribution (Fig 7) (75,76). (CLE may also be found in cigarette smokers with α_1 -antitrypsin deficiency.) Earlier stages of PLE are quite difficult to identify at CT, and quantitative CT may be preferred.

Paraseptal Emphysema

Heard (77) used the term *paraseptal emphysema* (PSE) to describe emphysematous lesions caused by selective destruction of the distal acinus (Fig 2, D), and subsequent reports have used it to describe lesions located near the pleural surface close to the chest wall and in the interlobar fissures. In some cases, multiple destroyed acini coalesce to form striking lesions just under the pleural surface on CT scans. Its relative frequency in radiology-based

studies like COPDGene suggest that it has been underappreciated in studies of postmortem and surgically resected lungs, perhaps because these specimens are rarely properly inflated before being examined. However, PSE is often not associated with significant symptoms or physiologic impairment (4).

PSE is characterized at CT by subpleural and peribronchovascular foci of low attenuation separated by intact interlobular septa thickened by associated mild fibrosis (78) (Figs 8, 9). PSE has a special predilection for peripheral subpleural lobules along the mediastinal and peripheral pleura and fissures, usually most marked in the middle and upper lungs and along the mediastinum. CT shows subpleural areas of low attenuation with a well-defined wall. Rows of PSE may mimic honeycombing, but the size of the cysts is larger than that of honeycomb cysts and architectural distortion and other signs of fibrosis are not present. In our experience, PSE is commonly associated with marked thickening of the walls of proximal bronchi and bronchioles, suggesting a significant airway inflammatory component. PSE occurs across the entire spectrum of minimal involvement to severe parenchymal obstruction and can be progressive. Because minimal subpleural emphysematous abnormality is quite common even in nonsmokers (79,80), it is reasonable to ignore or discount the presence of up to four or five small cysts (≤ 1 cm) at the lung apices.

Bullae (avascular low-attenuation areas >1 cm in diameter, with a thin but perceptible wall) are found in all types of emphysema (81) but are most commonly associated with PSE. Bullae are often located in the upper lobes in both CLE and PSE but are more evenly distributed in the lungs of patients with advanced destructive emphysema (76). Bullae may be large enough to cause reduced expansion of the adjacent lung parenchyma, which may sometimes result in sufficient atelectasis to appear as a masslike opacity (82). The term *giant bullous emphysema* has been used to describe the presence of bullae occupying at least one-third of a hemithorax (83).

Figure 8

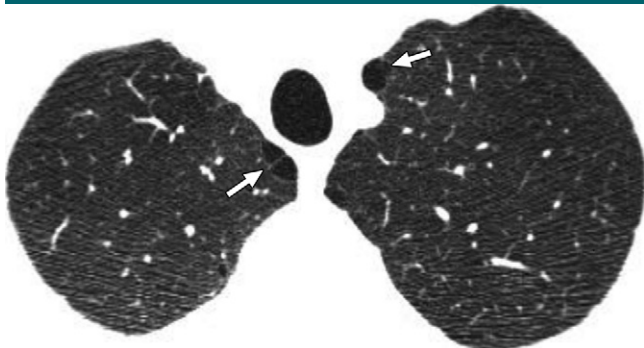


Figure 8: Mild PSE. CT scan in smoker without COPD shows subpleural foci of low attenuation separated by intact interlobular septa along the mediastinum (arrows), measuring less than 1 cm.

Figure 9

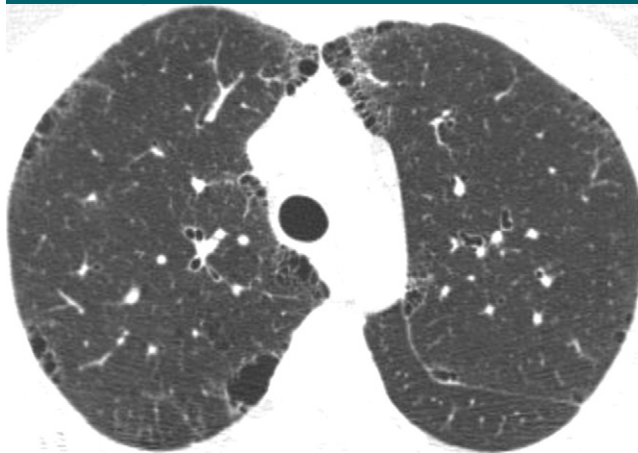


Figure 9: Substantial PSE. CT scan in patient with GOLD stage I COPD shows numerous well-demarcated areas of subpleural emphysema along chest wall and mediastinal pleural margins.

Figure 10

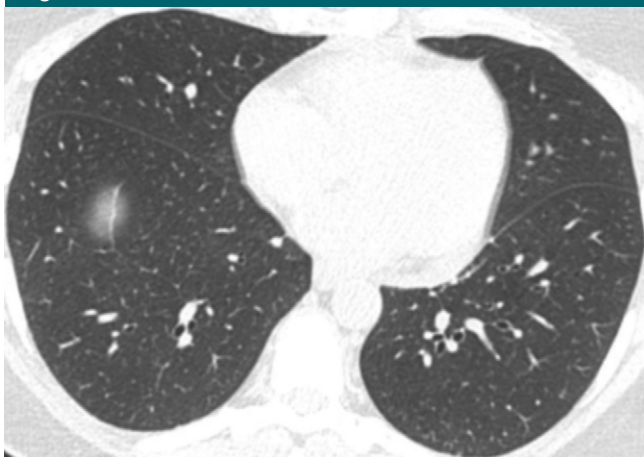


Figure 10: Normal bronchial walls. CT scan in asymptomatic nonsmoker with normal spirometric findings demonstrates normal airways.

Figure 11



Figure 11: Bronchial wall thickening. CT scan in cigarette smoker demonstrates marked thickening of segmental and subsegmental airways but no emphysema.

Bronchial Wall Thickening

Bronchial wall thickening is commonly observed in heavy cigarette smokers (84), particularly those with chronic bronchitis, presumably because of bronchial inflammation and remodeling. It may be visually identified at CT by a relative increase in bronchial wall thickness compared with the bronchial lumen and with the diameter of adjacent pulmonary arteries (85); however, this CT feature is subjective and associated with substantial interobserver variation (80,86). It is probably best assessed by comparison with visual standards obtained

from subjects with normal (Fig 10) and abnormal (Fig 11) findings (27).

Quantitative CT of airway dimensions is less subjective than visual evaluation. Quantitative CT of subsegmental airway dimensions can provide an estimate of small airway remodeling (87), probably because the same pathophysiologic process that causes small airway obstruction also takes place in large airways.

Increased thickness of airway walls is associated with the presence of

COPD (88), with reversibility of airway obstruction (89), and with symptoms of chronic bronchitis (90). In patients with COPD, bronchial wall thickening is an important independent predictor of FEV₁ (91,92) and of the risk of acute exacerbation (13).

Small Airways Disease

Cigarette smoking has distinct effects on the small airways that may be visible both pathologically and at CT. Niewoehner et al (93) showed that a characteristic form

Figure 12

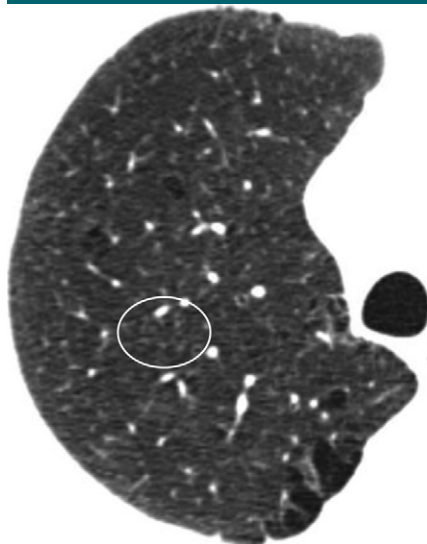


Figure 12: Widespread small centrilobular nodules. Centrilobular nodules (circled) in cigarette smoker are suggestive of respiratory bronchiolitis. Mild CLE and PSE are also present.

of respiratory bronchiolitis was present in the lungs of young persons who died suddenly outside the hospital. Although most of these lesions were observed in smokers, they were also found in non-smokers. The authors postulated that this form of bronchiolitis was a precursor to CLE. Myers et al (94) reported a similar but more severe form of respiratory bronchiolitis as the only finding at lung biopsies performed in six patients with clinical and radiologic evidence of interstitial lung disease. That was confirmed by other authors (95). Respiratory bronchiolitis is dominated by infiltrating mononuclear cells containing large numbers of macrophages with brown to black “smokers” inclusion bodies that stain positively with periodic acid Schiff and iron stains. These inclusions are thought to be based on abnormal lysosomal function of macrophages in smokers (96). Respiratory bronchiolitis is also commonly found in lung specimens removed as a treatment for lung cancer (97). The decrease in FEV_1 in COPD has also been related to a persistent infiltration of inflammatory immune cells into the walls of purely conducting airways, with a tendency to form tertiary lymphoid organs in the later

stages of COPD (98). A decrease in FEV_1 has also been associated with a reduction in terminal bronchiolar number and thickening of the walls of the bronchi that survive (7). Collectively, these data suggest that the region of the lung where the smaller purely conducting airways transition into respiratory bronchioles, alveolar ducts, and sacs is susceptible to the inhalation of a variety of toxic particles and gases, primarily but not exclusively derived from tobacco smoking.

Small airway disease is often an important major component of both emphysema-predominant disease and airway-predominant disease involving larger airways (bronchi). Isolated small airway disease can also occur as a primary expression of COPD. Physiologic identification of small airway disease is difficult. CT can be helpful in identifying signs of inflammatory small airway disease and small airway obstruction.

Inflammatory small airway disease.—Inflammation in and around the small airways in patients with COPD can cause the airways to become visible at CT as poorly defined centrilobular nodules of ground-glass attenuation (Fig 12) (99–101). Pathologically, this process commonly corresponds with respiratory bronchiolitis (24). CLE and bronchial wall thickening are frequent associated findings. The centrilobular nodules of respiratory bronchiolitis may progress to CLE (102). Unless it is severe, centrilobular nodularity is a subjective visual finding and the boundary between normal and abnormal may be difficult to set. For this reason, substantial observer variation has been found in the assessment of centrilobular nodularity (73). The small centrilobular nodules of respiratory bronchiolitis are sometimes associated with patchy areas of ground-glass opacity that reflect respiratory bronchiolitis–interstitial lung disease or desquamative interstitial pneumonia (100).

Obstructive small airway disease.—Obstructive small airway disease, in the absence of significant emphysema (defined in this analysis as quantitative CT extent of low-attenuation area <6%) may be identified by finding gas trapping at expiratory CT and/or by identifying physiologic obstruction (low FEV_1 with low

FEV_1/FVC consistent with GOLD grades II, III, and IV).

At expiratory CT in healthy subjects, the lung attenuation usually increases in a homogeneous fashion. Air trapping, recognized as patchy or diffuse preservation of lung attenuation at expiratory CT (Fig 13), is common in cigarette smokers (12,103–106). Mechanisms of air trapping identified at CT may include prolonged lung emptying because of bronchiolar narrowing and dropout (7) and/or emphysematous destruction with loss of the elastic recoil force required to drive air out of the lungs (17,107).

The resistance in the small conducting airways smaller than 2 mm in diameter accounts for only 10%–20% of total lower airway resistance in healthy subjects (108–110). In lungs affected by COPD, however, small airway resistance increases substantially (109,110)—particularly in subjects with COPD who have minimal emphysematous destruction (110). Micro-CT has shown that the number of terminal bronchioles is reduced to as little as 10% of control values in the end stage of the CLE phenotype of COPD and to 25% of control values in the end stage of the PLE phenotype of COPD (7). This degree of reduction in numbers of terminal bronchioles probably makes a very important contribution to the increase in small airways resistance in COPD.

Other Important CT Features in Cigarette Smokers and in COPD

Interstitial Lung Abnormalities

In addition to centrilobular nodules, CT scans obtained in cigarette smokers may show abnormalities compatible with infiltrative lung disease, including ground-glass and reticular abnormalities. In a study of 2416 COPD Gene participants who were cigarette smokers, an interstitial lung abnormality was found in 194 subjects (8%) (111). The prevalence of an interstitial abnormality increased with age, tobacco exposure, and current smoking. Although the interstitial abnormalities were usually asymptomatic, subjects with an interstitial

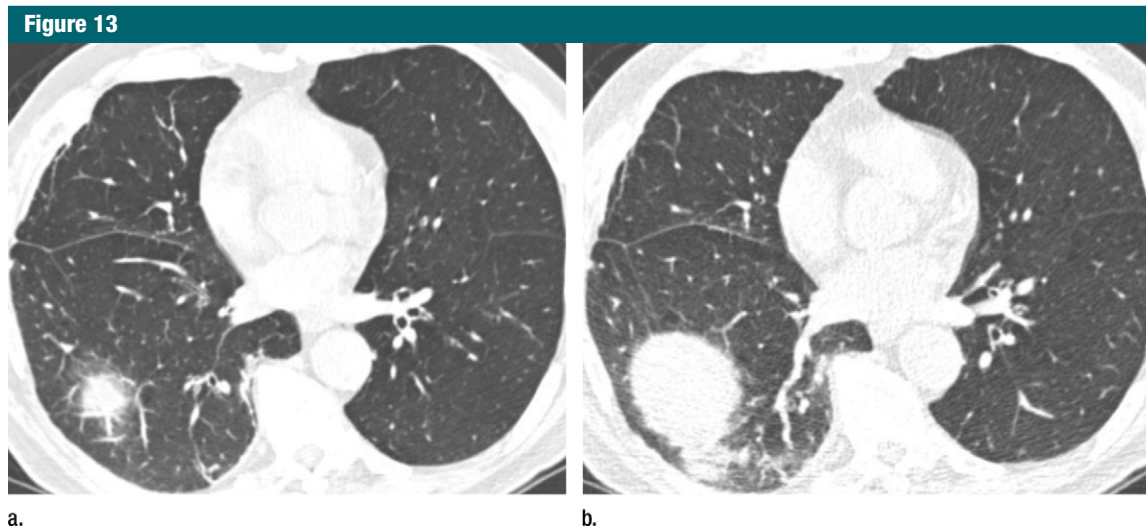


Figure 13: Gas trapping at expiratory CT. (a) Inspiratory and (b) expiratory CT scans in patient with severe airway obstruction (GOLD stage III) but only minimal emphysema. Lung attenuation fails to increase on expiratory scan, which is indicative of diffuse gas trapping owing to small airway obstruction.

abnormality were more likely to have a restrictive lung deficit and were less likely to meet the GOLD criteria for COPD. Similar changes were also seen in 2563 cigarette smokers in the MESA Lung Study and in the National Lung Screening Trial (112,113). Although detailed pathologic correlation is not available, these interstitial abnormalities likely correspond to variable combinations of respiratory bronchiolitis, airspace enlargement with fibrosis, and smoking-related interstitial fibrosis (114–116).

Pulmonary Vascular Disease

Pulmonary hypertension can be a complication of advanced COPD and may be due to hypoxic vasoconstriction, pulmonary vascular obliteration, sleep apnea, or left heart abnormality. This important comorbidity is an important predictor of hospitalization and death in COPD (117). Pulmonary hypertension can be identified at CT with the ratio of the diameters of the pulmonary artery and aorta (118,119). Enlargement of the pulmonary artery as determined by a pulmonary artery–aorta ratio of more than 1 was recently shown to be an independent risk factor for exacerbations in patients with COPD (120).

Abnormalities of the Trachea and Central Bronchi

Tracheobronchomalacia, defined as a reduction in the tracheal luminal cross-sectional area by more than 80% at dynamic expiratory imaging, is found in about 20% of patients with COPD but is not correlated with physiologic impairment (39). Indeed, the degree of tracheal collapse at end expiration in patients with COPD does not appear to be significantly different from that of control subjects (121). However, narrowing of the trachea in the coronal plane (saber-sheath trachea) is associated with COPD—particularly with more advanced stages of COPD (121–123). Diverticula or outpouching from the central airways may also be present; although the prevalence of bronchial diverticula is not different in patients with COPD than in control subjects (124), an increased number of diverticula is associated with a history of cigarette smoking (125) and with symptoms of cough (126).

Bronchiectasis

Bronchiectasis is defined at CT as a dilated bronchial lumen relative to the adjacent pulmonary artery, lack of bronchial tapering, or identification

of bronchi within 1 cm of the pleural surface (81). The reported prevalence of bronchiectasis at CT in subjects with COPD ranges from 27% (127,128) to 58% (129). Differences in prevalence may relate to differing populations and the variation in criteria for the diagnosis of bronchiectasis. Bronchiectasis is most commonly cylindrical in character (129). The presence of bronchiectasis is associated with more severe airflow obstruction and with hospital admission for exacerbation (129).

Summary

Integration of visual characterization of emphysema and airway abnormalities with physiologic and quantitative CT assessment permits categorization of COPD into distinct structurally and functionally defined subtypes. These include identification of patients with five different patterns of emphysema-predominant subtypes and two patterns of airway-predominant subtypes (Fig 14). In addition, quantitative CT analysis is important to determine the severity of emphysema and the magnitude of expiratory gas trapping. The subjectivity of visual determinations of emphysema severity and gas trapping suggests that the combination of visual scoring and

Figure 14

Emphysema (>6 % of pixels < -950 HU by QCT and/or visual identification of emphysema)*

Mild Centrilobular Emphysema (Mild CLE)

Upper Lobe Predominant

Moderate CLE

Upper Lobe Predominant
Diffuse

Confluent Emphysema (Con)

Upper Lobe Predominant
Diffuse

Advanced Destructive Emphysema (ADE)

Diffuse
Lower Lobe Predominant

Panlobular Emphysema (PLE)

A1AT Deficiency Related – Commonly
Lower Lobe Predominant

Paraseptal Emphysema (PSE)

Airway -Predominant Disease (<6 % of pixels < -950 HU by QCT)

Bronchial Disease

Small Airway Disease

Figure 14: CT-defined subtypes of COPD. Most subjects with emphysema have significant airway disease. Airway-predominant disease represents subjects with minimal or no emphysema as defined at quantitative CT (QCT). * = There is a group of subjects without visually defined emphysema who have more than 6% of pixels less than -950 HU at quantitative CT. Further work is needed to understand the importance of this finding, and these individuals cannot currently be classified. A1AT = α_1 -antitrypsin.

quantitative CT is essential to define these structure- and/or function-based COPD subtypes. Visual and quantitative CT evaluation will identify a substantial amount of disease in subjects with mild or absent physiologic evidence of airway obstruction. Use of consistent CT technique is required to characterize and quantify COPD subtypes in a manner that can help determine the progression of specific patterns of disease over time.

Clearly, this classification must be regarded as a work in progress, and a number of areas can be identified for future research, including observer variation of the visual classification system, outcomes of the CT-defined phenotypes,

histologic correlations of CT patterns, effect of aging on visual and quantitative features in the lung, CT phenotyping of nonsmoking-related COPD (eg, COPD related to biomass fuel), and clinical importance of increased quantitative measures of emphysema in subjects without visual emphysema.

Acknowledgments: We are grateful to Dragos Vasilescu, PhD, and Stijn Verleden, PhD, for preparing the images in Figure 2.

Disclosures of Conflicts of Interest: D.A.L. Activities related to the present article: disclosed no relevant relationships. Activities not related to the present article: is a paid consultant for Perceptice Imaging, Boehringer Ingelheim, Genetech, Gilead, and Intermune; received a grant from Centocor and Siemens. Other relationships: disclosed no relevant relationships. J.H.M.A. disclosed no relevant relationships. J.C.H. disclosed no relevant relationships. P.A.G. disclosed no relevant relationships. H.U.K. Activities related to the present article: disclosed no relevant relationships. Activities not related to the present article: received a grant from Siemens and Boehringer Ingelheim; receives personal fees for being on speakers bureau from Siemens, Boehringer Ingelheim, Bracco, Bayer, Novartis, and Almirall; is on the board at Siemens; receives fees from Siemens for the provision and evaluation of hardware and software; received fees from Boehringer Ingelheim for expert testimony; received fees from Boehringer Ingelheim for educational presentation. Other relationships: disclosed no relevant relationships. A.A.B. Activities related to the present article: disclosed no relevant relationships. Activities not related to the present article: is a paid consultant for Spiration and Olympus; receives payment for lectures including service on speakers bureaus from ATS; receives royalties from Elsevier. Other relationships: disclosed no relevant relationships. R.G.B. Activities related to the present article: disclosed no relevant relationships. Activities not related to the present article: received a grant from Alpha 1 Foundation; received royalties from UpToDate. Other relationships: disclosed no relevant relationships. T.V.C. disclosed no relevant relationships. J.R.G. disclosed no relevant relationships. P.A.G. disclosed no relevant relationships. H.C. Activities related to the present article: disclosed no relevant relationships. Activities not related to the present article: is a paid consultant for GSK; has grants/grants pending from GSK and Spiration. Other relationships: disclosed no relevant relationships. E.A.H. Activities related to the present article: disclosed no relevant relationships. Activities not related to the present article: is a member of the CT Advisory Board of Siemens Healthcare; is a paid consultant for GSK and Novartis. Other relationships: has patents with VIDA diagnostics through the University of Iowa; is founder and shareholder of VIDA Diagnostics. J.D.N. Activities related to the present article: disclosed no relevant relationships. Activities not related to the present article: is a paid consultant for VIDA Diagnostics and GlaxoSmithKline; has stock options in VIDA Diagnostics; received a grant from Roche Pharma-

ceutical and Siemens Healthcare. Other relationships: has a patent with VIDA Diagnostics. M.P. disclosed no relevant relationships. E.K.S. Activities related to the present article: disclosed no relevant relationships. Activities not related to the present article: received a grant and personal fees from GlaxoSmithKline; received personal fees from Merck; received travel expenses from Novartis. Other relationships: disclosed no relevant relationships. J.D.C. disclosed no relevant relationships.

References

- Petty TL, Weinmann GG. Building a national strategy for the prevention and management of and research in chronic obstructive pulmonary disease. National Heart, Lung, and Blood Institute Workshop Summary. Bethesda, Maryland, August 29–31, 1995. *JAMA* 1997;277(3):246–253.
- Fabbri LM, Hurd SS; GOLD Scientific Committee. Global strategy for the diagnosis, management and prevention of COPD: 2003 update. *Eur Respir J* 2003;22(1):1–2.
- Friedlander AL, Lynch D, Dyar LA, Bowler RP. Phenotypes of chronic obstructive pulmonary disease. *COPD* 2007;4(4):355–384.
- Smith BM, Austin JH, Newell JD Jr, et al. Pulmonary emphysema subtypes on computed tomography: the MESA COPD study. *Am J Med* 2014;127(1):94.e7–e23.
- Klein JS, Gamsu G, Webb WR, Golden JA, Müller NL. High-resolution CT diagnosis of emphysema in symptomatic patients with normal chest radiographs and isolated low diffusing capacity. *Radiology* 1992;182(3):817–821.
- Mets OM, Schmidt M, Buckens CF, et al. Diagnosis of chronic obstructive pulmonary disease in lung cancer screening computed tomography scans: independent contribution of emphysema, air trapping and bronchial wall thickening. *Respir Res* 2013;14(1):59.
- McDonough JE, Yuan R, Suzuki M, et al. Small-airway obstruction and emphysema in chronic obstructive pulmonary disease. *N Engl J Med* 2011;365(17):1567–1575.
- Müller NL, Staples CA, Miller RR, Abboud RT. “Density mask:” an objective method to quantitate emphysema using computed tomography. *Chest* 1988;94(4):782–787.
- Murata K, Itoh H, Todo G, et al. Centrilobular lesions of the lung: demonstration by high-resolution CT and pathologic correlation. *Radiology* 1986;161(3):641–645.
- Madani A, Zanen J, de Maertelaer V, Gevenois PA. Pulmonary emphysema: objective quantification at multi-detector row CT—comparison with macroscopic and microscopic morphometry. *Radiology* 2006;238(3):1036–1043.

11. Coxson HO, Rogers RM, Whittall KP, et al. A quantification of the lung surface area in emphysema using computed tomography. *Am J Respir Crit Care Med* 1999; 159(3):851–856.
12. Schroeder JD, McKenzie AS, Zach JA, et al. Relationships between airflow obstruction and quantitative CT measurements of emphysema, air trapping, and airways in subjects with and without chronic obstructive pulmonary disease. *AJR Am J Roentgenol* 2013;201(3):W460–W470.
13. Han MK, Bartholmai B, Liu LX, et al. Clinical significance of radiologic characterizations in COPD. *COPD* 2009;6(6):459–467.
14. Johannessen A, Skorge TD, Bottai M, et al. Mortality by level of emphysema and airway wall thickness. *Am J Respir Crit Care Med* 2013;187(6):602–608.
15. Galbán CJ, Han MK, Boes JL, et al. Computed tomography-based biomarker provides unique signature for diagnosis of COPD phenotypes and disease progression. *Nat Med* 2012;18(11):1711–1715.
16. Mets OM, Buckens CF, Zanen P, et al. Identification of chronic obstructive pulmonary disease in lung cancer screening computed tomographic scans. *JAMA* 2011; 306(16):1775–1781.
17. Gevenois PA, De Vuyst P, Sy M, et al. Pulmonary emphysema: quantitative CT during expiration. *Radiology* 1996;199(3): 825–829.
18. Mohamed Hoesein FA, Schmidt M, Mets OM, et al. Discriminating dominant computed tomography phenotypes in smokers without or with mild COPD. *Respir Med* 2014;108(1):136–143.
19. Fain SB, Panth SR, Evans MD, et al. Early emphysematous changes in asymptomatic smokers: detection with 3He MR imaging. *Radiology* 2006;239(3):875–883.
20. Gierada DS, Woods JC, Jacob RE, et al. Emphysema quantification in inflation-fixed lungs using low-dose computed tomography and 3He magnetic resonance imaging. *J Comput Assist Tomogr* 2010;34(5):773–779.
21. Lutey BA, Lefrak SS, Woods JC, et al. Hyperpolarized ³He MR imaging: physiologic monitoring observations and safety considerations in 100 consecutive subjects. *Radiology* 2008;248(2):655–661.
22. Sukstanskii AL, Yablonskiy DA. In vivo lung morphometry with hyperpolarized ³He diffusion MRI: theoretical background. *J Magn Reson* 2008;190(2):200–210.
23. Mugler JP 3rd, Altes TA. Hyperpolarized ¹²⁹Xe MRI of the human lung. *J Magn Reson Imaging* 2013;37(2):313–331.
24. Halaweish AF, Moon RE, Foster WM, et al. Perfluoropropane gas as a magnetic resonance lung imaging contrast agent in humans. *Chest* 2013;144(4):1300–1310.
25. Friedman PJ. Imaging studies in emphysema. *Proc Am Thorac Soc* 2008;5(4):494–500.
26. Remy-Jardin M, Remy J, Gosselin B, Copin MC, Wurtz A, Duhamel A. Sliding thin slab, minimum intensity projection technique in the diagnosis of emphysema: histopathologic-CT correlation. *Radiology* 1996;200(3):665–671.
27. Kim SS, Seo JB, Lee HY, et al. Chronic obstructive pulmonary disease: lobe-based visual assessment of volumetric CT by using standard images—comparison with quantitative CT and pulmonary function test in the COPDGene study. *Radiology* 2013; 266(2):626–635.
28. Mayo JR. CT evaluation of diffuse infiltrative lung disease: dose considerations and optimal technique. *J Thorac Imaging* 2009; 24(4):252–259.
29. Sieren JP, Newell JD, Judy PF, et al. Reference standard and statistical model for intersite and temporal comparisons of CT attenuation in a multicenter quantitative lung study. *Med Phys* 2012;39(9):5757–5767.
30. Parr DG, Stoel BC, Stolk J, Nightingale PG, Stockley RA. Influence of calibration on densitometric studies of emphysema progression using computed tomography. *Am J Respir Crit Care Med* 2004;170(8):883–890.
31. Newell JD Jr, Sieren J, Hoffman EA. Development of quantitative computed tomography lung protocols. *J Thorac Imaging* 2013;28(5):266–271.
32. Sieren J, Hoffman EA, Baumhauer H, et al. CT imaging protocol standardization for use in a multicenter study: SPIROMICS [abstr]. In: Radiological Society of North America Scientific Assembly and Annual Meeting Program. Oak Brook, Ill: Radiological Society of North America, 2011; 262.
33. Gierada DS, Bierhals AJ, Choong CK, et al. Effects of CT section thickness and reconstruction kernel on emphysema quantification relationship to the magnitude of the CT emphysema index. *Acad Radiol* 2010;17(2):146–156.
34. Ley-Zaporozhan J, Ley S, Weinheimer O, et al. Quantitative analysis of emphysema in 3D using MDCT: influence of different reconstruction algorithms. *Eur J Radiol* 2008;65(2):228–234.
35. Tschirren J, Hoffman EA, McLennan G, Sonka M. Segmentation and quantitative analysis of intrathoracic airway trees from computed tomography images. *Proc Am Thorac Soc* 2005;2(6):484–487, 503–504.
36. Lo P, van Ginneken B, Reinhardt JM, et al. Extraction of airways from CT (EXACT'09). *IEEE Trans Med Imaging* 2012; 31(11):2093–2107.
37. Mets OM, Willemink MJ, de Kort FP, et al. The effect of iterative reconstruction on computed tomography assessment of emphysema, air trapping and airway dimensions. *Eur Radiol* 2012;22(10):2103–2109.
38. Hersh CP, Washko GR, Estépar RS, et al. Paired inspiratory-expiratory chest CT scans to assess for small airways disease in COPD. *Respir Res* 2013;14(1):42.
39. Boiselle PM, Michaud G, Roberts DH, et al. Dynamic expiratory tracheal collapse in COPD: correlation with clinical and physiologic parameters. *Chest* 2012;142(6):1539–1544.
40. Kalender WA, Riemüller R, Seissler W, Behr J, Welke M, Fichte H. Measurement of pulmonary parenchymal attenuation: use of spirometric gating with quantitative CT. *Radiology* 1990;175(1):265–268.
41. Fuld MK, Grout RW, Guo J, Morgan JH, Hoffman EA. Systems for lung volume standardization during static and dynamic MDCT-based quantitative assessment of pulmonary structure and function. *Acad Radiol* 2012;19(8):930–940.
42. Bankier AA, O'Donnell CR, Boiselle PM. Quality initiatives: respiratory instructions for CT examinations of the lungs: a hands-on guide. *RadioGraphics* 2008;28(4):919–931.
43. Ley-Zaporozhan J, Ley S, Krummenauer F, Ohno Y, Hatabu H, Kauczor HU. Low dose multi-detector CT of the chest (iLEAD Study): visual ranking of different simulated mAs levels. *Eur J Radiol* 2010;73(2):428–433.
44. Gietema HA, Müller NL, Fauerbach PV, et al. Quantifying the extent of emphysema: factors associated with radiologists' estimations and quantitative indices of emphysema severity using the ECLIPSE cohort. *Acad Radiol* 2011;18(6):661–671.
45. Zaporozhan J, Ley S, Weinheimer O, et al. Multi-detector CT of the chest: influence of dose onto quantitative evaluation of severe emphysema: a simulation study. *J Comput Assist Tomogr* 2006;30(3):460–468.
46. Madani A, De Maertelaer V, Zanen J, Gevenois PA. Pulmonary emphysema: radiation dose and section thickness at multidetector CT quantification—comparison with macroscopic and microscopic morphometry. *Radiology* 2007;243(1):250–257.
47. Regan EA, Hokanson JE, Murphy JR, et al. Genetic epidemiology of COPD (COPD-Gene) study design. *COPD* 2010;7(1):32–43.
48. Coxson HO, Dirksen A, Edwards LD, et al. The presence and progression of emphysema in COPD as determined by CT scanning and biomarker expression: a prospective analysis from the ECLIPSE study. *Lancet Respir Med* 2013;1(2):129–136.
49. Vestbo J, Anderson W, Coxson HO, et al. Evaluation of COPD longitudinally to identify predictive surrogate end-points (ECLIPSE). *Eur Respir J* 2008;31(4):869–873.

50. Couper D, LaVange LM, Han M, et al. Design of the subpopulations and intermediate outcomes in copd study (SPIROMICS). *Thorax* 2014;69(5):491–494.
51. Bankier AA, Schaefer-Prokop C, De Maertelaer V, et al. Air trapping: comparison of standard-dose and simulated low-dose thin-section CT techniques. *Radiology* 2007;242(3):898–906.
52. Nishio M, Matsumoto S, Ohno Y, et al. Emphysema quantification by low-dose CT: potential impact of adaptive iterative dose reduction using 3D processing. *AJR Am J Roentgenol* 2012;199(3):595–601.
53. Zach JA, Newell JD Jr, Schroeder J, et al. Quantitative computed tomography of the lungs and airways in healthy nonsmoking adults. *Invest Radiol* 2012;47(10):596–602.
54. Hackx M, Bankier AA, Gevenois PA. Chronic obstructive pulmonary disease: CT quantification of airways disease. *Radiology* 2012;265(1):34–48.
55. Lee YK, Oh YM, Lee JH, et al. Quantitative assessment of emphysema, air trapping, and airway thickening on computed tomography. *Lung* 2008;186(3):157–165.
56. Paré PD, Nagano T, Coxson HO. Airway imaging in disease: gimmick or useful tool? *J Appl Physiol* (1985) 2012;113(4):636–646.
57. Xie X, de Jong PA, Oudkerk M, et al. Morphological measurements in computed tomography correlate with airflow obstruction in chronic obstructive pulmonary disease: systematic review and meta-analysis. *Eur Radiol* 2012;22(10):2085–2093.
58. Lynch DA, Al-Qaisi MA. Quantitative computed tomography in chronic obstructive pulmonary disease. *J Thorac Imaging* 2013;28(5):284–290.
59. McLean K. The histology of localized emphysema. *Australasian annals of medicine*. 1957;6(4):282–294.
60. McLean K. The histology of generalized pulmonary emphysema. II. Diffuse emphysema. *Australas Ann Med* 1957;6(3):203–217.
61. McLean KH. The histology of generalized pulmonary emphysema. I. The genesis of the early centrilobular lesion: focal emphysema. *Australas Ann Med* 1957;6(2):124–140.
62. McLean KH. The macroscopic anatomy of pulmonary emphysema. *Australas Ann Med* 1956;5(2):73–88.
63. Leopold JG, Gough J. The centrilobular form of hypertrophic emphysema and its relation to chronic bronchitis. *Thorax* 1957;12(3):219–235.
64. Leopold JG, Gough J. Post-mortem bronchography in the study of bronchitis and emphysema. *Thorax* 1963;18:172–177.
65. Hogg JC, Nepszy SJ, Macklem PT, Thurlbeck WM. Elastic properties of the centrilobular emphysematous space. *J Clin Invest* 1969;48(7):1306–1312.
66. Foster WL Jr, Gimenez EI, Roubidoux MA, et al. The emphysemas: radiologic-pathologic correlations. *Radiographics* 1993;13(2):311–328.
67. Foster WL Jr, Pratt PC, Roggli VL, Godwin JD, Halvorsen RA Jr, Putman CE. Centrilobular emphysema: CT-pathologic correlation. *Radiology* 1986;159(1):27–32.
68. Hruban RH, Meziane MA, Zerhouni EA, et al. High resolution computed tomography of inflation-fixed lungs: pathologic-radiologic correlation of centrilobular emphysema. *Am Rev Respir Dis* 1987;136(4):935–940.
69. Kim WD, Eidelman DH, Izquierdo JL, Ghezzi H, Saetta MP, Cosio MG. Centrilobular and panlobular emphysema in smokers: two distinct morphologic and functional entities. *Am Rev Respir Dis* 1991;144(6):1385–1390.
70. Wyatt JP, Fischer VW, Sweet HC. Panlobular emphysema: anatomy and pathodynamics. *Dis Chest* 1962;41(3):239–259.
71. Laurell CB, Eriksson S. The electrophoretic α_1 -globulin pattern of serum in α_1 -antitrypsin deficiency. *Scand J Clin Lab Invest* 1963;15(2):132–140.
72. Perlmutter DH, Brodsky JL, Balistreri WF, Trapnell BC. Molecular pathogenesis of alpha-1-antitrypsin deficiency-associated liver disease: a meeting review. *Hepatology* 2007;45(5):1313–1323.
73. Lehman A, Mattman A, Sin D, et al. Emphysema in an adult with galactosialidosis linked to a defect in primary elastic fiber assembly. *Mol Genet Metab* 2012;106(1):99–103.
74. Stern EJ, Frank MS, Schmutz JF, Glenn RW, Schmidt RA, Godwin JD. Panlobular pulmonary emphysema caused by i.v. injection of methylphenidate (ritalin): findings on chest radiographs and CT scans. *AJR Am J Roentgenol* 1994;162(3):555–560.
75. Copley SJ, Wells AU, Müller NL, et al. Thin-section CT in obstructive pulmonary disease: discriminatory value. *Radiology* 2002;223(3):812–819.
76. Guest PJ, Hansell DM. High resolution computed tomography (HRCT) in emphysema associated with alpha-1-antitrypsin deficiency. *Clin Radiol* 1992;45(4):260–266.
77. Heard BE. A pathological study of emphysema of the lungs with chronic bronchitis. *Thorax* 1958;13(2):136–149.
78. Satoh K, Kobayashi T, Misao T, et al. CT assessment of subtypes of pulmonary emphysema in smokers. *Chest* 2001;120(3):725–729.
79. Mets OM, van Hulst RA, Jacobs C, van Ginneken B, de Jong PA. Normal range of emphysema and air trapping on CT in young men. *AJR Am J Roentgenol* 2012;199(2):336–340.
80. COPDGene CT Workshop Group, Barr RG, Berkowitz EA, et al. A combined pulmonary-radiology workshop for visual evaluation of COPD: study design, chest CT findings and concordance with quantitative evaluation. *COPD* 2012;9(2):151–159.
81. Hansell DM, Bankier AA, MacMahon H, McLoud TC, Müller NL, Remy J. Fleischner society: glossary of terms for thoracic imaging. *Radiology* 2008;246(3):697–722.
82. Gierada DS, Glazer HS, Slone RM. Pseudomass due to atelectasis in patients with severe bullous emphysema. *AJR Am J Roentgenol* 1997;168(1):85–92.
83. Stern EJ, Webb WR, Weinacker A, Müller NL. Idiopathic giant bullous emphysema (vanishing lung syndrome): imaging findings in nine patients. *AJR Am J Roentgenol* 1994;162(2):279–282.
84. Park JS, Brown KK, Tuder RM, Hale VA, King TE Jr, Lynch DA. Respiratory bronchiolitis-associated interstitial lung disease: radiologic features with clinical and pathologic correlation. *J Comput Assist Tomogr* 2002;26(1):13–20.
85. Ooi GC, Khong PL, Chan-Yeung M, et al. High-resolution CT quantification of bronchiectasis: clinical and functional correlation. *Radiology* 2002;225(3):663–672.
86. Grenier P, Mourey-Gerosa I, Benali K, et al. Abnormalities of the airways and lung parenchyma in asthmatics: CT observations in 50 patients and inter- and intraobserver variability. *Eur Radiol* 1996;6(2):199–206.
87. Nakano Y, Wong JC, de Jong PA, et al. The prediction of small airway dimensions using computed tomography. *Am J Respir Crit Care Med* 2005;171(2):142–146.
88. Berger P, Perot V, Desbarats P, Tunon-de-Lara JM, Marthan R, Laurent F. Airway wall thickness in cigarette smokers: quantitative thin-section CT assessment. *Radiology* 2005;235(3):1055–1064.
89. Kitaguchi Y, Fujimoto K, Kubo K, Honda T. Characteristics of COPD phenotypes classified according to the findings of HRCT. *Respir Med* 2006;100(10):1742–1752.
90. Orlandi I, Moroni C, Camiciottoli G, et al. Chronic obstructive pulmonary disease: thin-section CT measurement of airway wall thickness and lung attenuation. *Radiology* 2005;234(2):604–610.
91. Aziz ZA, Wells AU, Desai SR, et al. Functional impairment in emphysema: contribution of airway abnormalities and distribution of parenchymal disease. *AJR Am J Roentgenol* 2005;185(6):1509–1515.
92. Hasegawa M, Nasuhara Y, Onodera Y, et al. Airflow limitation and airway dimensions in chronic obstructive pulmonary disease. *Am J Respir Crit Care Med* 2005;171(2):142–146.

- nary disease. *Am J Respir Crit Care Med* 2006;173(12):1309–1315.
93. Niewoehner DE, Kleinerman J, Rice DB. Pathologic changes in the peripheral airways of young cigarette smokers. *N Engl J Med* 1974;291(15):755–758.
 94. Myers JL, Veal CF Jr, Shin MS, Katzenstein AL. Respiratory bronchiolitis causing interstitial lung disease: a clinicopathologic study of six cases. *Am Rev Respir Dis* 1987;135(4):880–884.
 95. Yousem SA, Colby TV, Gaensler EA. Respiratory bronchiolitis-associated interstitial lung disease and its relationship to desquamative interstitial pneumonia. *Mayo Clin Proc* 1989;64(11):1373–1380.
 96. Monick MM, Powers LS, Walters K, et al. Identification of an autophagy defect in smokers' alveolar macrophages. *J Immunol* 2010;185(9):5425–5435.
 97. Hogg JC, Wright JL, Wiggs BR, Coxson HO, Opazo Saez A, Paré PD. Lung structure and function in cigarette smokers. *Thorax* 1994;49(5):473–478.
 98. Hogg JC, Chu F, Utokaparch S, et al. The nature of small-airway obstruction in chronic obstructive pulmonary disease. *N Engl J Med* 2004;350(26):2645–2653.
 99. Gruden JF, Webb WR. CT findings in a proved case of respiratory bronchiolitis. *AJR Am J Roentgenol* 1993;161(1):44–46.
 100. Heyneman LE, Ward S, Lynch DA, Remy-Jardin M, Johkoh T, Müller NL. Respiratory bronchiolitis, respiratory bronchiolitis-associated interstitial lung disease, and desquamative interstitial pneumonia: different entities or part of the spectrum of the same disease process? *AJR Am J Roentgenol* 1999;173(6):1617–1622.
 101. Okada F, Ando Y, Yoshitake S, et al. Clinical/pathologic correlations in 553 patients with primary centrilobular findings on high-resolution CT scan of the thorax. *Chest* 2007;132(6):1939–1948.
 102. Remy-Jardin M, Edme JL, Boulenguez C, Remy J, Mastora I, Sobaszek A. Longitudinal follow-up study of smoker's lung with thin-section CT in correlation with pulmonary function tests. *Radiology* 2002;222(1):261–270.
 103. Crausman RS, Ferguson G, Irvin CG, Make B, Newell JD Jr. Quantitative chest computed tomography as a means of predicting exercise performance in severe emphysema [published correction appears in *Acad Radiol* 1995;2(10):870]. *Acad Radiol* 1995;2(6):463–469.
 104. Eda S, Kubo K, Fujimoto K, Matsuzawa Y, Sekiguchi M, Sakai F. The relations between expiratory chest CT using helical CT and pulmonary function tests in emphysema. *Am J Respir Crit Care Med* 1997;155(4):1290–1294.
 105. Lee KW, Chung SY, Yang I, Lee Y, Ko EY, Park MJ. Correlation of aging and smoking with air trapping at thin-section CT of the lung in asymptomatic subjects. *Radiology* 2000;214(3):831–836.
 106. Matsuoka S, Kurihara Y, Yagihashi K, Hoshino M, Watanabe N, Nakajima Y. Quantitative assessment of air trapping in chronic obstructive pulmonary disease using inspiratory and expiratory volumetric MDCT. *AJR Am J Roentgenol* 2008;190(3):762–769.
 107. Mead J, Turner JM, Macklem PT, Little JB. Significance of the relationship between lung recoil and maximum expiratory flow. *J Appl Physiol* 1967;22(1):95–108.
 108. Macklem PT, Mead J. Resistance of central and peripheral airways measured by a retrograde catheter. *J Appl Physiol* 1967;22(3):395–401.
 109. Hogg JC, Macklem PT, Thurlbeck WM. Site and nature of airway obstruction in chronic obstructive lung disease. *N Engl J Med* 1968;278(25):1355–1360.
 110. Yanai M, Sekizawa K, Ohri T, Sasaki H, Takishima T. Site of airway obstruction in pulmonary disease: direct measurement of intrabronchial pressure. *J Appl Physiol* (1985) 1992;72(3):1016–1023.
 111. Washko GR, Lynch DA, Matsuoka S, et al. Identification of early interstitial lung disease in smokers from the COPDGene study. *Acad Radiol* 2010;17(1):48–53.
 112. Jin GY, Lynch D, Chawla A, et al. Interstitial lung abnormalities in a CT lung cancer screening population: prevalence and progression rate. *Radiology* 2013;268(2):563–571.
 113. Lederer DJ, Enright PL, Kawut SM, et al. Cigarette smoking is associated with subclinical parenchymal lung disease: the Multi-Ethnic Study of Atherosclerosis (MESA)-lung study. *Am J Respir Crit Care Med* 2009;180(5):407–414.
 114. Reddy TL, Mayo J, Churg A. Respiratory bronchiolitis with fibrosis: high-resolution computed tomography findings and correlation with pathology. *Ann Am Thorac Soc* 2013;10(6):590–601.
 115. Katzenstein AL, Mukhopadhyay S, Zanardi C, Dexter E. Clinically occult interstitial fibrosis in smokers: classification and significance of a surprisingly common finding in lobectomy specimens. *Hum Pathol* 2010;41(3):316–325.
 116. Yamada T, Nakanishi Y, Homma T, et al. Airspace enlargement with fibrosis shows characteristic histology and immunohistology different from usual interstitial pneumonia, nonspecific interstitial pneumonia and centrilobular emphysema. *Pathol Int* 2013;63(4):206–213.
 117. Chaouat A, Naeije R, Weitzenblum E. Pulmonary hypertension in COPD. *Eur Respir J* 2008;32(5):1371–1385.
 118. Murray TI, Boxt LM, Katz J, Reagan K, Barst RJ. Estimation of pulmonary artery pressure in patients with primary pulmonary hypertension by quantitative analysis of magnetic resonance images. *J Thorac Imaging* 1994;9(3):198–204.
 119. Ng CS, Wells AU, Padley SP. A CT sign of chronic pulmonary arterial hypertension: the ratio of main pulmonary artery to aortic diameter. *J Thorac Imaging* 1999;14(4):270–278.
 120. Wells JM, Washko GR, Han MK, et al. Pulmonary arterial enlargement and acute exacerbations of COPD. *N Engl J Med* 2012;367(10):913–921.
 121. Lee HJ, Seo JB, Chae EJ, et al. Tracheal morphology and collapse in COPD: correlation with CT indices and pulmonary function test. *Eur J Radiol* 2011;80(3):e531–e535.
 122. Greene R, Lechner GL. "Saber-sheath" trachea: a clinical and functional study of marked coronal narrowing of the intrathoracic trachea. *Radiology* 1975;115(2):265–268.
 123. Gupta PP, Yadav R, Verma M, Agarwal D, Kumar M. Correlation between high-resolution computed tomography features and patients' characteristics in chronic obstructive pulmonary disease. *Ann Thorac Med* 2008;3(3):87–93.
 124. Higuchi T, Takahashi N, Shiotani M, et al. Main bronchial diverticula in the subcarinal region: their relation to airflow limitations. *Acta Radiol* 2012;53(1):44–48.
 125. Miyara T, Oshiro Y, Yamashiro T, Kamiya H, Ogawa K, Murayama S. Bronchial diverticula detected by multidetector-row computed tomography: incidence and clinical features. *J Thorac Imaging* 2011;26(3):204–208.
 126. Sverzellati N, Ingegnoli A, Calabrò E, et al. Bronchial diverticula in smokers on thin-section CT. *Eur Radiol* 2010;20(1):88–94.
 127. Bafadhel M, Umar I, Gupta S, et al. The role of CT scanning in multidimensional phenotyping of COPD. *Chest* 2011;140(3):634–642.
 128. O'Brien C, Guest PJ, Hill SL, Stockley RA. Physiological and radiological characterization of patients diagnosed with chronic obstructive pulmonary disease in primary care. *Thorax* 2000;55(8):635–642.
 129. Martínez-García MA, Soler-Cataluña JJ, Donat Sanz Y, et al. Factors associated with bronchiectasis in patients with COPD. *Chest* 2011;140(5):1130–1137.